

Supporting Information

Stabilizing BiOCl/Ti₃C₂T_x Hybrids for Potassium-Ion Batteries via Solid Electrolyte Interphase Reconstruction

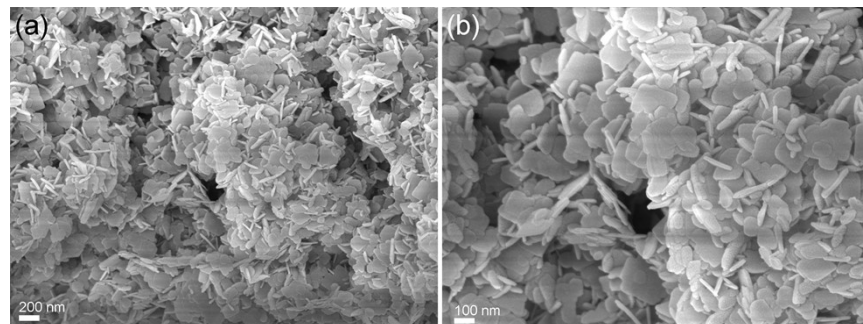


Figure S1. (a, b) SEM images of bare BiOCl nanosheets.

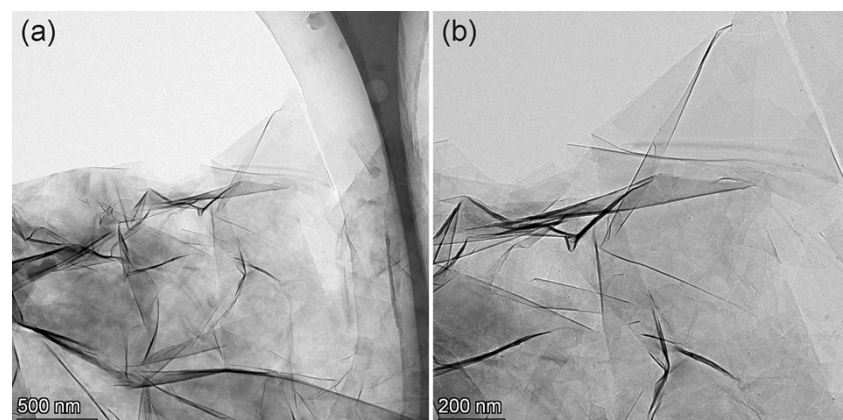


Figure S2. (a, b) TEM images of Ti₃C₂T_x nanosheets.

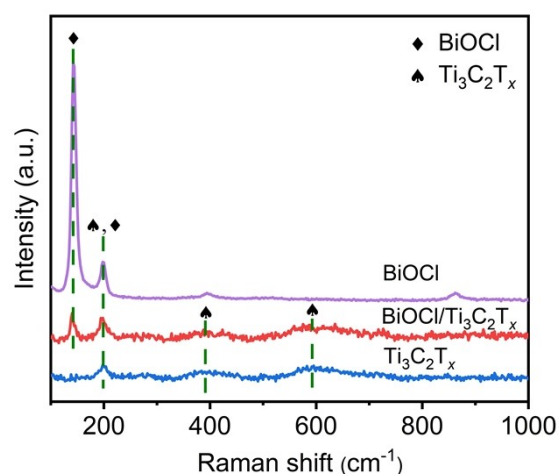


Figure S3. Raman spectra of BiOCl, BiOCl/Ti₃C₂T_x, and Ti₃C₂T_x.

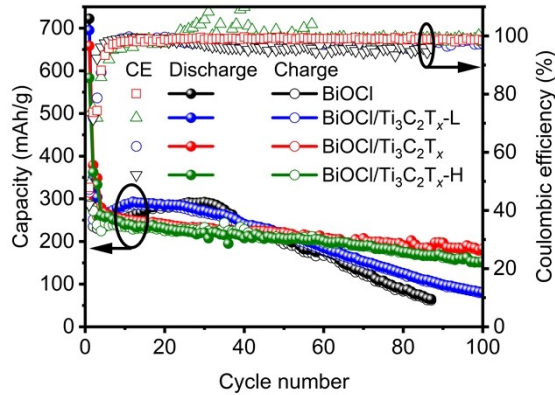


Figure S4. Cycling performances and Coulombic efficiencies of $\text{BiOCl}/\text{Ti}_3\text{C}_2\text{T}_x$ composites at 50 mA/g in the electrolyte of DME-KFSI-5.

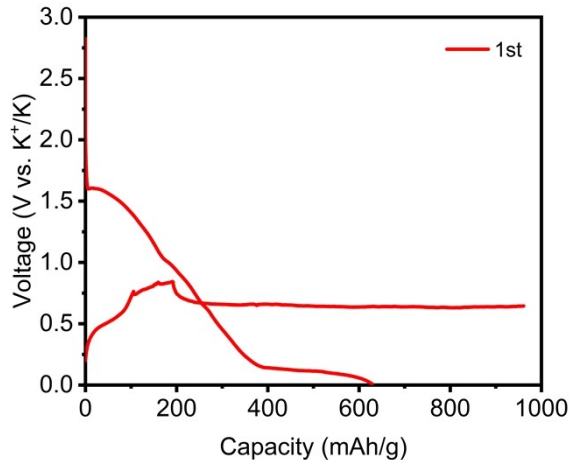


Figure S5. GCD curves of $\text{BiOCl}/\text{Ti}_3\text{C}_2\text{T}_x$ in the DME-KFSI-1 electrolyte.

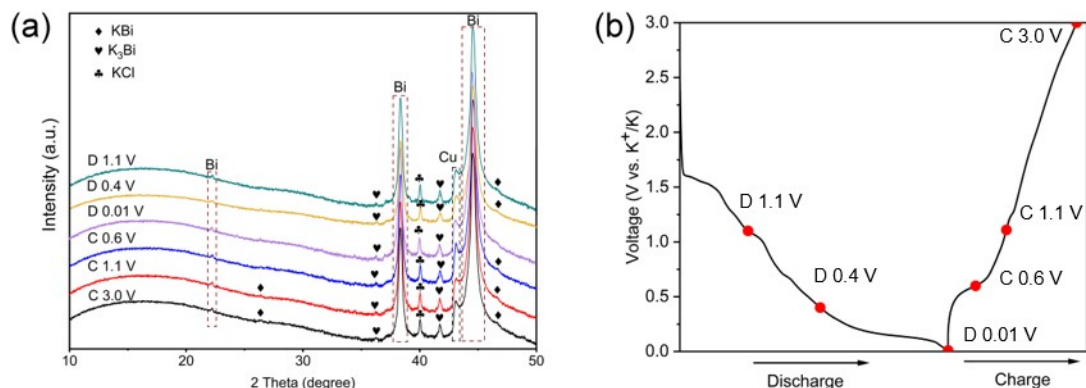


Figure S6. (a) *Ex-situ* XRD patterns of the $\text{BiOCl}/\text{Ti}_3\text{C}_2\text{T}_x$ electrodes at various discharge/charge states. (b) Discharge/charge profiles of $\text{BiOCl}/\text{Ti}_3\text{C}_2\text{T}_x$ in the first cycle.

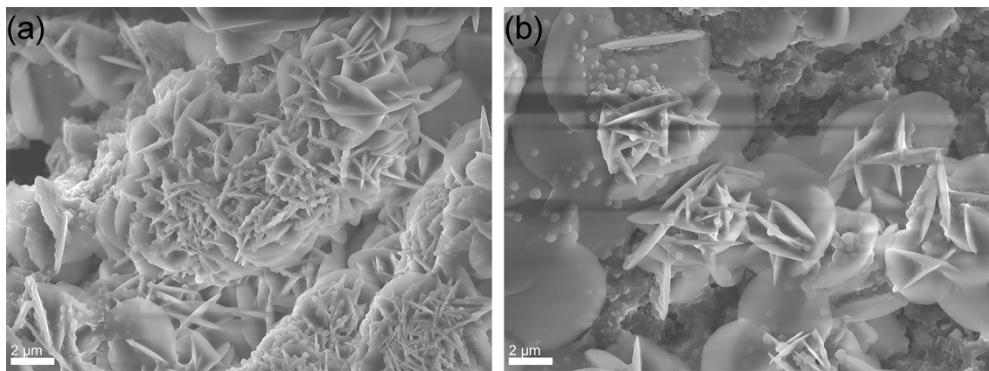


Figure S7. (a, b) SEM images of the $\text{BiOCl}/\text{Ti}_3\text{C}_2\text{T}_x$ electrode after 5 cycles.

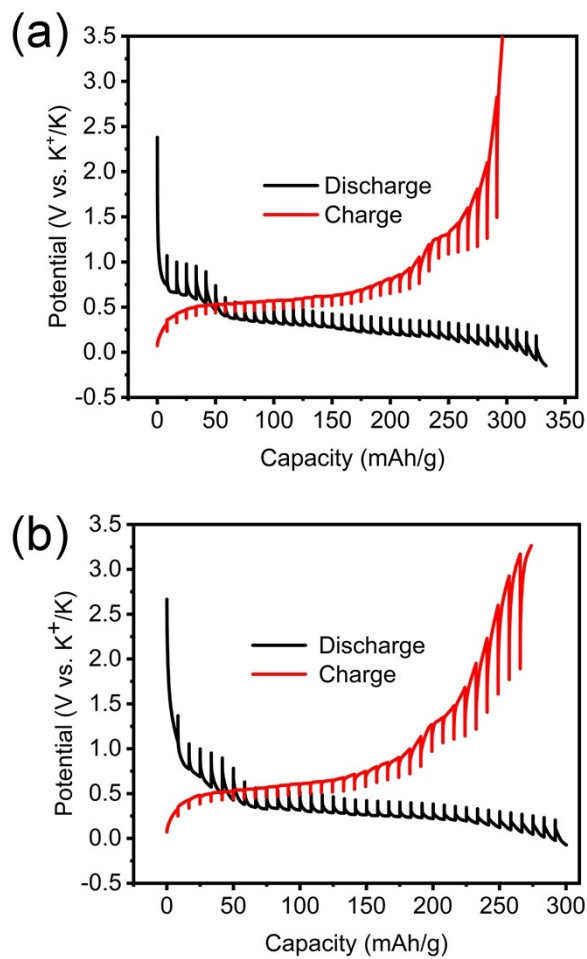


Figure S8. GITT curves of the cells with (a) BiOCl and (b) $\text{BiOCl}/\text{Ti}_3\text{C}_2\text{T}_x$ electrodes at a current density of 50 mA/g in the electrolyte of DME-KFSI-5.

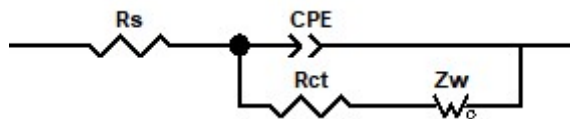


Figure S9. Electrochemical equivalent circuit model for fitting Nyquist plots.

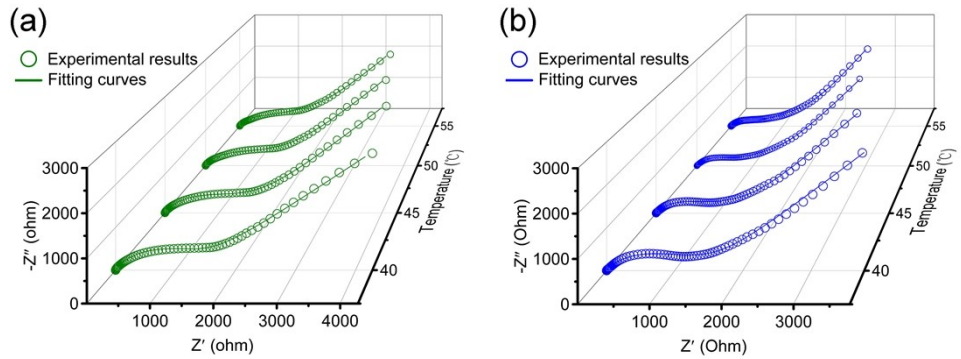


Figure S10. Temperature-dependent Nyquist plots for $\text{BiOCl}/\text{Ti}_3\text{C}_2\text{T}_x$ in (a) ED-KPF and DME-KFSI-3 electrolytes.

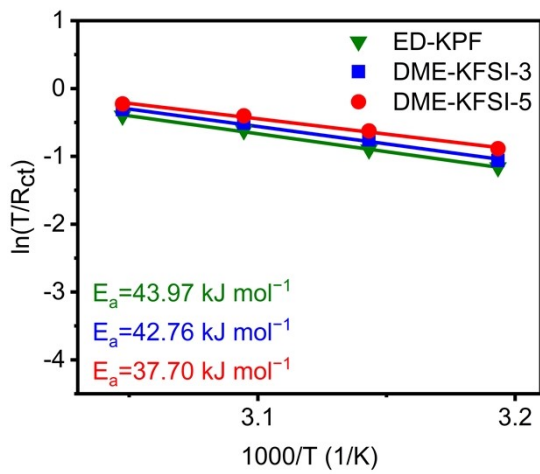


Figure S11. Plots of $\ln(T/R_{\text{ct}})$ vs. $1000/T$ with the derived activation energies for $\text{BiOCl}/\text{Ti}_3\text{C}_2\text{T}_x$ in different electrolytes.

Table S1. Comparison of the electrochemical performance of reported anodes for PIBs.

Materials	Current density (mA/g)	Capacity (mAh/g)	Cycle number	Electrolyte system	Ref.
Bi@C	10	151	35	5 M KTFSI in DGM	1
BiOCl nanoflake	50	213	50	1 M KFSI in EC: DEC (1:1, v/v)	2
Bi/rGO	50	87	200	1 M KFSI in EC: DEC (1:1, v/v)	3
Sn foil	50	66	300	1 M KPF ₆ in EC: DMC: EMC (4:3:2 v/v/v)	4
Nanoporous Ge	20	120	400	0.5 M KPF ₆ in EC: DEC (1:1, v/v)	5
MXene nanosheet	100	50	100	1 M KPF ₆ in PC: EC (1:1, w/w)	6
Ti ₃ C ₂					
Titanium carbonitride	20	75	100	0.8 M KPF ₆ in EC: DEC (1:1, v/v)	7
Ti ₃ CNT _z					
Reduced graphene oxide film	10	145	100	0.8 M KPF ₆ in EC: DEC (1:1, v/v)	8
Sn ₃ P ₄ /C	50	10	120	0.8 M KPF ₆ in EC: DEC (1:1, v/v)	9
BiOCl/Ti ₃ C ₂ T _x	50	184	100	5 M KFSI in DME	This work

Table S2. Calculated R_{ct} based on the equivalent circuits via fitting the impedance spectra at different temperatures.

Samples	Electrolyte system	R _{ct} (Ω)			
		40 °C	45 °C	50 °C	55 °C
BiOCl	5 M KFSI in DME	5449	4319	3194	2313
	0.8 M KPF ₆ in EC: DEC (1:1, v/v)	1022	783.3	599.2	489.6
BiOCl/Ti ₃ C ₂ T _x	3 M KFSI in DME	905.2	678.4	539.5	477.3
	5 M KFSI in DME	759.4	594.6	483.1	411.2

Table S3. Density functional theory calculation results.

Electrolyte	Compound	LUMO (eV)	HOMO (eV)
DME EC: DEC	FSI ⁻	0.94	-7.14
	DME	2.30	-6.92
	PF ₆ ⁻	3.01	-8.99
	EC	0.83	-8.23
	DEC	1.02	-7.90

References

1. R. D. Zhang, J. Z. Bao, Y. H. Wang and C. F. Sun, Concentrated electrolytes stabilize bismuth-potassium batteries, *Chem. Sci.*, 2018, **9**, 6193-6198.
2. W. Li, Y. Xu, Y. L. Dong, Y. H. Wu, C. L. Zhang, M. Zhou, Q. Fu, M. H. Wu and Y. Lei, Bismuth oxychloride nanoflake assemblies as a new anode for potassium ion batteries, *Chem. Commun.*, 2019, **55**, 6507-6510.
3. Q. Zhang, J. F. Mao, W. K. Pang, T. Zheng, V. Sencadas, Y. Z. Chen, Y. J. Liu and Z. P. Guo, Boosting the Potassium Storage Performance of Alloy-Based Anode Materials via Electrolyte Salt Chemistry, *Adv. Energy Mater.*, 2018, **8**, 1703288.
4. B. F. Ji, F. Zhang, X. H. Song and Y. B. Tang, A Novel Potassium-Ion-Based Dual-Ion Battery, *Adv. Mater.*, 2017, **29**, 1700519.
5. Q. Yang, Z. F. Wang, W. Xi and G. He, Tailoring nanoporous structures of Ge anodes for stable potassium-ion batteries, *Electrochem. Commun.*, 2019, **101**, 68-72.
6. Y. Xie, Y. Dall'Agnese, M. Naguib, Y. Gogotsi, M. W. Barsoum, H. L. L. Zhuang and P. R. C. Kent, Prediction and Characterization of MXene Nanosheet Anodes for Non-Lithium-Ion Batteries, *ACS Nano*, 2014, **8**, 9606-9615.
7. M. Naguib, R. A. Adams, Y. P. Zhao, D. Zemlyanov, A. Varma, J. Nanda and V. G. Pol, Electrochemical performance of MXenes as K-ion battery anodes, *Chem. Commun.*, 2017, **53**, 6883-6886.
8. W. Luo, J. Y. Wan, B. Ozdemir, W. Z. Bao, Y. N. Chen, J. Q. Dai, H. Lin, Y. Xu, F. Gu, V. Barone and L. B. Hu, Potassium Ion Batteries with Graphitic Materials, *Nano Lett.*, 2015, **15**, 7671-7677.
9. W. C. Zhang, J. F. Mao, S. A. Li, Z. X. Chen and Z. P. Guo, Phosphorus-Based Alloy Materials for Advanced Potassium-Ion Battery Anode, *J. Am. Chem. Soc.*, 2017, **139**, 3316-3319.